



## Novel pore-filled polyelectrolyte composite membranes for cathodic microbial fuel cell application

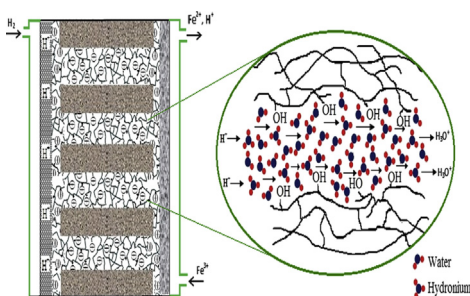
J.M. Gohil, D.G. Karamanov\*

Department of Chemical and Biochemical Engineering, Western University, London, Ontario N6A 5B9, Canada

### HIGHLIGHTS

- Novel PVA pore-filled polycarbonate proton exchange membrane.
- Investigation of membrane physiochemical properties with PVA cross-link time.
- Pore-filled membranes showed very good performance and stability.
- Microbial fuel cell eliminates Pt catalyst at cathode and Nafion membrane use.

### GRAPHICAL ABSTRACT



### ARTICLE INFO

#### Article history:

Received 19 March 2013

Received in revised form

11 May 2013

Accepted 1 June 2013

Available online 11 June 2013

#### Keywords:

Pore-filled membrane

Poly(vinyl alcohol)

Microbial fuel cell

Cross-linking

Biogenerator

### ABSTRACT

Novel pore-filled polyelectrolyte membrane (PEM) was produced using track etched polycarbonate (PC) as porous substrate and poly(vinyl alcohol) (PVA) as pore filling material. PVA in PC pores was stabilized through cross-linking of PVA matrix with glutaraldehyde (GA). Cross-link time was varied from 24 h to 96 h while keeping the membranes in GA solution. Pore sizes of substrate PC membrane tested were 0.01, 0.1 and 0.2 μm. The membranes were characterized by Fourier-transform infrared spectroscopy and scanning electron microscopy. Ionic conductivity, water uptake, contact angle and gel content have been measured to determine membranes performance. The ionic crossover (iron ions and protons) through membranes was studied in a complete fuel cell. The single-cell performance of membrane was tested in a cathodic microbial fuel cell (MFC, Biogenerator). The physicochemical properties and membranes fuel cell performance were highly depended on the cross-link density of PVA matrices. Membranes cross-linked with GA for 72 h showed maximum gel content and their peak power density has reached 110 mW cm<sup>-2</sup> at current density of 378 mA cm<sup>-2</sup>. Among all, membrane cross-linked for 72 h was studied for continuous long-term stability, which showed consistency for application in MFC.

Crown Copyright © 2013 Published by Elsevier B.V. All rights reserved.

### 1. Introduction

Polymer electrolyte or proton exchange membranes (PEMs) have gained considerable attention due to their applications in energy related fields such as fuel cells and battery systems. The specific applications of fuel cells depend on the type of fuel cell

used. In general, fuel cells are capable of producing power anywhere in the range between a fraction of 1 W to 10 MW scale for automotive, stationary and portable power applications [1]. Basically, a polymer electrolyte membrane fuel cell (PEMFC) creates electrical power from chemical energy by direct continuous conversion of an externally supplied fuel and oxidant. In conventional fuel cells, hydrogen rich oxidizable fuel, hydrogen, methanol, ethanol or formic acid used as proton source, and oxygen used as oxidant. PEMFC can be categorized according to type of electrolyte employed. Among other polymers, PVA has been tested as a cross-

\* Corresponding author. Tel.: +1 519 661 2111x88230; fax: +1 519 661 3498.

E-mail address: [dkaraman@uwo.ca](mailto:dkaraman@uwo.ca) (D.G. Karamanov).



linked PEM in conventional H<sub>2</sub>/O<sub>2</sub> and direct methanol fuel cell (DMFC) applications due to its excellent film forming characteristics and reactive chemical functions favorable for physicochemical modifications [2]. In order to increase mechanical stability and decrease excessive swelling of PVA membranes, cross-linking through chemical treatment was performed. Many reagents explored as cross-linking agents, including glutaraldehyde (GA), provided good control of cross-linking to produce water stable PVA membranes [3–5]. The controlled swelling of membrane may provide porosity for the transport of protons and thereby increase the mobility of protonic charge carrier, leading to slightly increased proton conductivities. Moreover water swollen PVA can be easily doped with H<sub>3</sub>PO<sub>4</sub>/H<sub>2</sub>SO<sub>4</sub> which provides conduction path [6]. Beside that other monomers, oligomers or polymers containing negative charge were often combined with PVA to increase its proton conductivity [2]. Philip and Hsu have systematically studied PVA film membrane preparations through cross-linking by acetalization through GA or periodic acid and by irradiation method [3]. Shen et al. [7] prepared GA cross-linked sulfonated PVA (sPVA) polymer matrix for PEM. Cross-linked sPVA membranes with high degree of sulfonation (DS) exhibited higher conductivity ( $1.4 \times 10^{-3}$  S cm<sup>-1</sup>) than membranes with a low DS (proton conductivity of  $0.96 \times 10^{-3}$  S cm<sup>-1</sup>). Zeng et al. [8] reported sol–gel reaction approach between GA and PVA in an aqueous solution of phosphoric acid to fabricate phosphoric acid doped polyGA-H<sub>3</sub>PO<sub>4</sub>-PVA (PGA-PVA) hybrid amphibious PEMs. Kang et al. [9] examined blended systems of PVA/polystyrene sulfonic acid-co-maleic acid and GA as cross-linking agent to fabricate PEM for fuel cell.

Generally, cross-linked PVA membranes employed in fuel cell application are produced in composite form [7] because homogeneous PVA film membranes are not mechanically strong enough. A pore-filled composite PEM comprises a porous substrate and a polymer that fills the pores of the substrate. The pore-filled PEMs were prepared either via graft copolymerization from the base polymer (materials), by in situ polymerization or via cross-linking of presynthesized polymers [10]. Functional separation membranes, selective or responsive polymers that swell significantly in water or organic solvents can be mechanically stabilized by entrapment into the membranes pores (with or without anchoring to the wall). In pore-filled polyelectrolyte composite membranes, pore filling materials support proton conductivity while porous support prevents the excessive swelling through the pores walls and provides dimensional stability. For instance, the pore filling composite membranes concept reduced the reactant gas crossover in conventional H<sub>2</sub>/O<sub>2</sub> fuel cell [11,12] or methanol crossover in the case of DMFC [13,14] to improve its efficiency. In this respect, various combinations of porous substrate and pore filling polyelectrolyte have used in fuel cells application include: porous polytetrafluoroethylene (PTFE) and polyimide filled with Nafion ionomers, poly(vinyl sulfonic acid co-acrylic acid) or sulfonated polyether sulfone [14–17]; porous PTFE or polyvinylidene fluoride (PVDF) filled with polystyrene sulfonic acid or sulfonated polystyrene [18,19]; and microporous polyethylene impregnated with sulfonated hydrogenated butadiene–styrene block copolymer [20] etc.

The PVA swelling through interaction with aqueous electrolyte such as aqueous sulfuric acid solution allows a protonic charge transfer by the Grötthuss mechanism [21] through hydrogen-bonded sulfuric acid to hydroxyl groups of PVA. The excessive PVA swelling can be controlled by its entrapment into pores of inert substrate membranes. The main goals of the present study included the preparation and characterization of pore-filled composite PEM, which was more suitable for novel microbial fuel cell (MFCs) application. PVA was used as a pore filling material and a track etched PC membrane – as a porous substrate. The PVA was stabilized through cross-linking with GA. The cylindrical pores of the

track etched PC membrane provide short pathways for the protonic charge transfer. The pore-filled PEMs were characterized using Fourier-transform infrared (FTIR) and scanning electron microscopy (SEM). The membrane properties such as water uptake rate, proton conductivity, hydrophilicity and gel content were also determined. Pore-filled PEM described herein were employed in cathodic MFC [22]. Advantageously the MFC uses H<sub>2</sub> gas at anode and biologically produced ferric ion solution at the cathode, and eliminate the use of expensive Nafion PEM and Pt electrocatalyst at the cathode. This paper also shows the performance of the new MEA in a single-cell MFC.

## 2. Experimental

### 2.1. Materials

Sample of Elvanol® Polyvinyl alcohol (PVA) (Grade: 71–30; 99–99.8% hydrolyzed, Viscosity 27–33 mP S, 4% aqueous solution at 20 °C) was obtained from DuPont (USA). Glutaraldehyde (50 wt.%) was purchased from Caledon Laboratories Ltd. (Georgetown, Canada). Track etched polycarbonate (PC) membranes (pore size of 0.01, 0.1 and 0.2 µm) produced by GE Water & Processes Technologies, were purchased from Midland Scientific, Inc., (Omaha, USA).

### 2.2. Preparation of pore-filled PEM

The PVA solution (4 wt.%) was prepared in deionized water, and in order to ensure a complete dissolution of PVA, it was heated at 90 °C for 3–4 h. After the solution became clear, it was allowed to cool at room temperature. The solution was filtered off to remove any suspended particles. To prepare pore-filled PEM, the PVA solution was passed through the porous track etched PC membranes using a vacuum filter. The vacuum was applied until the porous membrane became impermeable to the liquid. After impregnation of porous PC membranes with PVA, they were dried for 24 h at room temperature. Further, the dried membranes were dip-coated at room temperature to form a thin layer of PVA on the surface of the PC membrane. The pores of PC membrane were chemically stabilized through cross-linking of PVA using GA as cross-linking agent. Dried PVA membranes were immersed into 0.2 M GA solution (GA solution prepared by diluting 50 wt.% aqueous solution using 0.5 M sodium sulphate solution and pH of solution adjusted to 3 by adding 1 M sulphuric acid solution). After certain time, membranes were lifted from cross-linking bath washed with deionized water to remove any traces of unreacted GA and stored in deionized water.

### 2.3. Membrane characterization

FTIR spectra of the samples were collected using Nicolet 6700 FT-IR spectrometer (Thermo Scientific, USA). PC, PVA film and pores filled PEMs samples were analyzed using Smart iTR accessory in transmittance mode in the range of wavenumber 4000–600 cm<sup>-1</sup> with resolution of 4 cm<sup>-1</sup>.

Top-view and cross-sectional microstructures of PC and PVA pore-filled PC membranes were examined under SEM (HITACHI S-2600N, Japan). The membranes samples were sputter coated with gold and analyzed at 5.0 kV accelerating voltage.

The ionic conductivity of PEMs was determined by a direct current two-point-probe method as described in Ref. [23]. The measuring cell consisted of four compartments. The auxiliary cathode and anode working compartments were used to apply an electrical field. The membrane under investigation was installed between the two central compartments that were separated from the auxiliary compartments by anion and cation exchange

membranes at the cathode and anode side respectively to prevent transport of water dissociation product formed at the working electrode to the central (working) compartments. The voltage drop across the studied membrane (active cross-sectional area  $11.3\text{ cm}^2$ ) was measured using Luggin capillaries facing the membranes surface. The capillaries were filled with saturated aqueous solution of potassium chloride ( $\text{KCl}_{\text{sat}}$ ) and each of them was connected to a test tube filled with  $\text{KCl}_{\text{sat}}$  having  $\text{Ag}/\text{AgCl}$ ,  $\text{KCl}_{\text{sat}}$  reference electrode in it. The reference electrodes were connected to a mV-meter (ORION 420A) for measuring the potential difference. The anode and cathode compartments were filled with 10% aqueous  $\text{H}_2\text{SO}_4$  solutions. The temperature was controlled at  $22^\circ\text{C}$ . During the measurement, the membrane samples were equilibrated with the working solutions during 24 h period. The solution in the auxiliary and a in the central compartment at the cathodic side was the same ( $1.09\text{ M H}_2\text{SO}_4$ ) for all the experiments, while the central anodic compartment was filled with the corresponding working solution. The voltage drop ( $\Delta U$ , mV) across the studied membrane was measured as a function of the current density ( $I$ ,  $\text{mA cm}^{-2}$ ) in the range  $0$ – $55\text{ mA cm}^{-2}$ , while stepwise increasing the current applied. The conductivity value ( $\sigma$ ,  $\text{mS cm}^{-1}$ ) of membrane was calculated as:

$$\sigma = L/RA \quad (1)$$

where  $L$  and  $A$  are the thickness (cm) and the active membrane area ( $\text{cm}^2$ ), respectively.  $R$  is the membrane resistance ( $\Omega$ ). The latter was calculated from the linear part of the  $I/\Delta U$  plots.

The water uptake (%) of pore-filled membrane was calculated as:

$$\text{Water uptake } (\%) = \frac{M_w - M_d}{M_d} \times 100 \quad (2)$$

where  $M_w$  and  $M_d$  are wet and dry weight of membrane, respectively. The membrane sample was kept in deionized water for 7 days before measuring the wet weight.

To measure the gel content (%), previously weighed dry membrane samples were immersed in 1 M sulphuric acid solution. After 7 days, the samples were taken out of the solution, washed with deionized water, dried in oven at  $70^\circ\text{C}$  for 24 h, and weighed. The gel content was calculated according to Eq. (3):

$$\text{Gel content } (\%) = \frac{M_{dw} - M_{dwl}}{M_{dw}} \times 100 \quad (3)$$

where  $M_{dw}$  and  $M_{dwl}$  are the dry weights of the membrane before and after leaching, respectively.

Static contact angle ( $\theta$ ,  $^\circ$ ) of membranes were determined using Axisymmetric Drop Shape Analyzer, FTA 1000 C Class (First Ten Angstroms, Portsmouth, VA, USA). Distilled water droplets were used as a contacting liquid with the membrane surface.

#### 2.4. Ionic crossover measurement

The major ionic components of the bioreactor solution are ferric ions ( $\text{Fe}^{+3}$ ) and sulphuric acid. Their crossover through membrane was measured in a complete fuel cell. The  $\text{H}_2$  gas leaving the anode was bubbled at constant flow rate through water to collect Fe ions and sulphuric acid from the liquid leaving the anode side. At each current density, the fuel cell was run continuously and after 1-h sample was collected. The concentrations of  $\text{Fe(III)}$  and  $\text{Fe(II)}$  ions were analyzed by UV–Visible spectrometer (Varian Cary 50 UV–Visible Spectrophotometer, Australia) according to the spectrophotometric method described in Ref. [24]. The concentration of sulphuric acid was determined by titration with standard solution

**Table 1**  
PC substrate properties and pore-filled membranes preparation conditions.

Membrane code	PC substrate membrane		PEMs cross-link time (h) <sup>a</sup>
	Pore size ( $\mu\text{m}$ )	Thickness ( $\mu\text{m}$ )	
PVAPC0	0.2	10	0
PVAPC1	0.2	10	24
PVAPC2	0.2	10	48
PVAPC3	0.2	10	72
PVAPC4	0.2	10	96
PVAPC5	0.1	6	72
PVAPC6	0.01	6	72

<sup>a</sup> Cross-linking bath contained 0.2 M GA in 0.5 M  $\text{Na}_2\text{SO}_4$  at pH of 3.

of dilute sodium hydroxide. The ionic crossover was calculated according to formula:

$$\text{Ionic crossover} = \frac{CV}{At} \quad (4)$$

where  $A$  is the membrane cross-sectional area ( $\text{cm}^2$ ),  $C$  is the total Fe ions or sulphuric acid concentration in water ( $\text{mol l}^{-1}$ ),  $t$  is time (s),  $V$  is the actual volume of the water sample (l).

#### 2.5. MEA preparation and single-cell test

PEMs performance was evaluated in microbial fuel cell (MBFCs) using a membrane electrode assembly (MEA). Cathode and anode comprised of porous activated graphite felt and platinized gas diffusion electrode (GDE) respectively. Commercial GDE used herein consists of carbon fabric and microporous layer. GDE coated with active Pt catalyst layer was combined with PVA pore-filled PC membrane. The active area of the MFC was  $5.29\text{ cm}^2$ . MEA single-cell performance evaluated using a conventional fuel cell with parallel serpentine flow-field on graphite plates. The bioreactor solution of  $0.45\text{ M Fe}_2(\text{SO}_4)_3$  containing  $\text{H}_2\text{SO}_4$  (pH 1) was pumped through the cathode compartment and hydrogen was supplied to the anode chamber. The cells were tested at  $22^\circ\text{C}$  with hydrogen at the anode side at pressure ( $\Delta P$ ) of  $10.1$ – $13.7\text{ kPa}$  (flow rate of  $0.55\text{ ml s}^{-1}$ ) and bioreactor solution circulated at  $35^\circ\text{C}$  at the cathode compartment with flow rate of  $2$ – $3\text{ ml s}^{-1}$ . The measurement of cell potential as a function of current density was conducted galvanostatically using Chroma DC electronic load.

#### 3. Working principle of cathodic MFC (Biogenerator)

The Biogenerator is a combined bio-electrochemical energy conversion system. It continuously produces electricity from hydrogen fuel and atmospheric oxygen in a combined electrochemical – bioreactor system. Cathodic MFC i.e. the Biogenerator comprises of

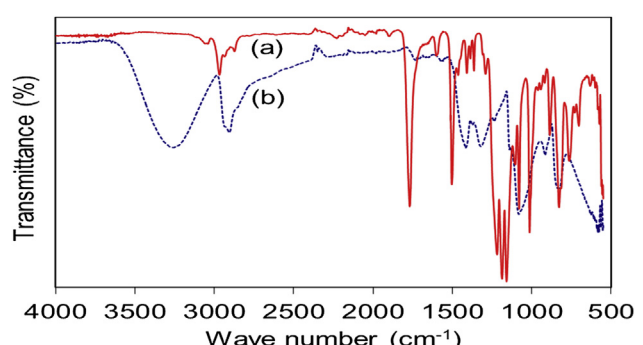
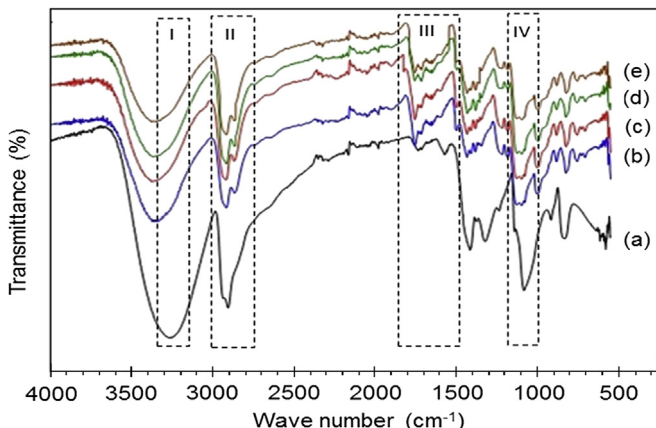


Fig. 1. FTIR spectra of (a) PC membrane (pore size  $0.2\text{ }\mu\text{m}$ ), and (b) PVA film.



**Fig. 2.** FTIR spectra of (a) pristine, and PVA pore-filled PEMs cross-linked with GA for (b) 24, (c) 48, (d) 72 and (e) 96 h.

two major units: PEMFC, and a bioreactor. The microorganisms in the bioreactor produce ferric ions, which have used as an oxidant in the cathode of the fuel cell unit. The fuel used was hydrogen gas.

#### 4. Results and discussion

##### 4.1. Membrane preparation

Pore filling approach of PC membranes showed that 4 wt.% PVA solution (viscosity of 27–33 mP S) was found appropriate to fill the

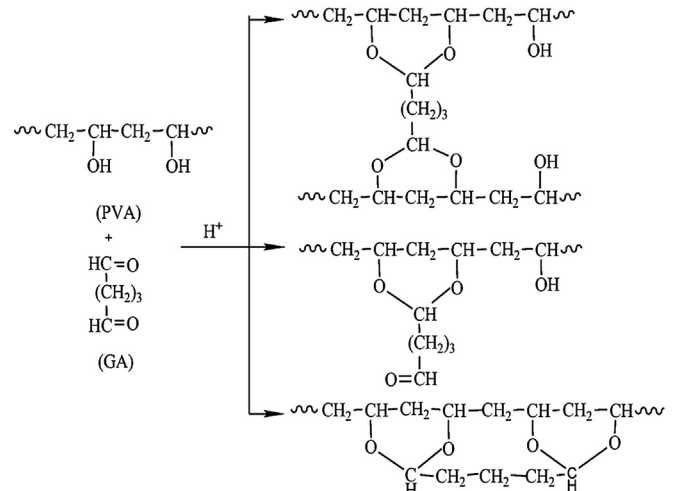


**Fig. 3.** Schematic of PVA and GA reaction.

porous substrate without the entrapment of air bubbles. Pristine PVA pore-filled membrane is the PEM prepared without GA cross-linking. PC substrate having pore size of 0.1 and 0.01 μm were also tested to prepare GA cross-linked PVA pore-filled membranes with the same fabrication technique keeping GA cross-linking time 72 h. The details of PEM preparation conditions and PC substrate membranes properties are shown in Table 1.

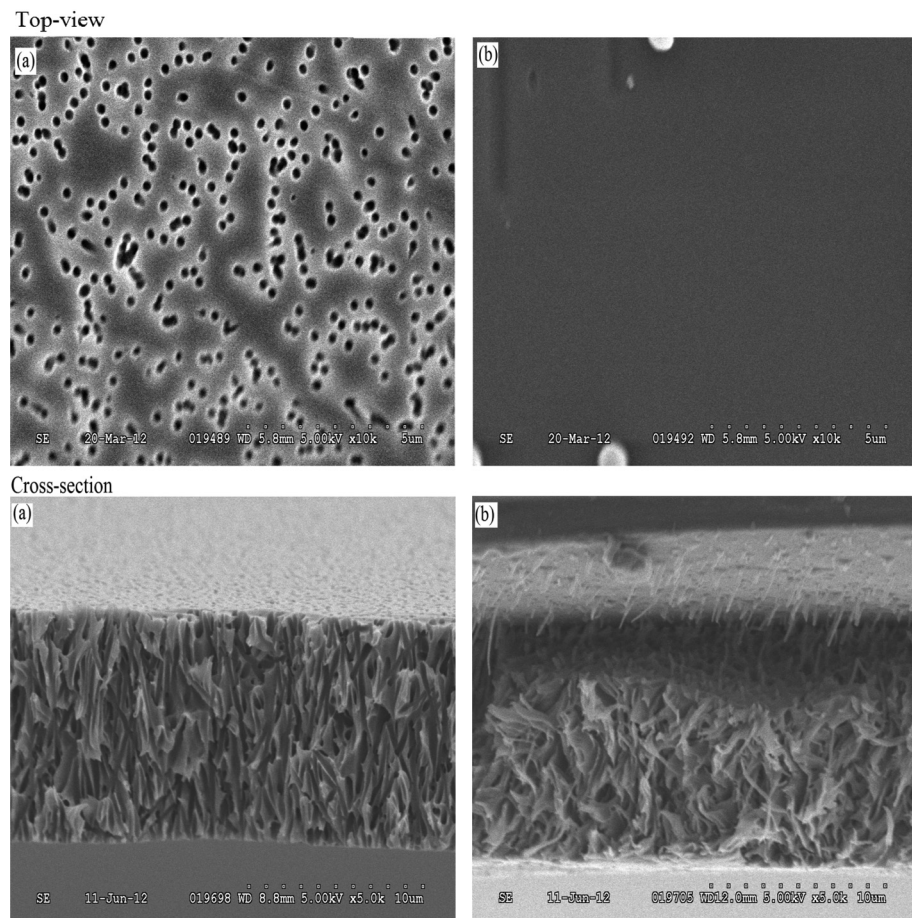


**Fig. 4.** SEM top-view and cross-sectional micrographs for (a) PC membrane, and (b) PVA filled membranes (PVAPC3).

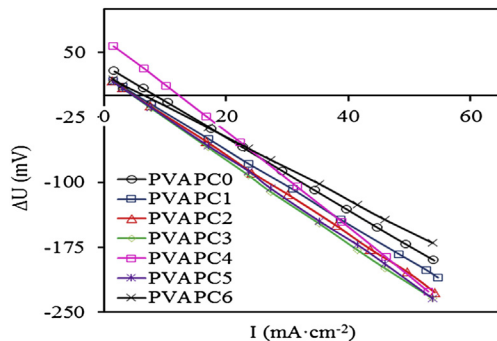


**Fig. 5.** The relationship between voltage drop and current density for pristine and GA cross-linked PVA pore-filled membranes.

In the pore-filled membranes for MFC the following criteria were used to compare their quality: (i) minimum iron crossover, (ii) minimum water uptake and maximum gel content, and (iii) stability in acidic solution (pH 1) while showing low swelling and high proton conductivity.

#### 4.2. FTIR study

Fig. 1a shows the ATR-IR spectrum of bare PC track etched membrane. The characteristics vibration and stretching bands observed for the PC membrane resemble those from bis(4-hydroxyphenyl)-2-propane, bisphenol A polycarbonate [25]. Fig. 1b represents the spectrum of dried PVA homogeneous film. The spectrum of dried PVA film is similar to that formed from fully hydrolyzed PVA [26]. The characteristic strong bands observed between 3500 and 3200 cm<sup>-1</sup> are linked to the stretching O-H from intermolecular and intramolecular hydrogen bonds. The C-H stretching vibration has been observed at 2934–2904 cm<sup>-1</sup>. The peaks at 1707 and 1096 cm<sup>-1</sup> are attributed to the stretching vibration of C=O and C-O of the remaining nonhydrolyzed vinyl acetate groups of the PVA. The peak at 1378 cm<sup>-1</sup> is due to –CH<sub>2</sub>– wagging and that at 1328 cm<sup>-1</sup> is due to –C-H– and –O-H– bending [27].

Fig. 2 represents the spectra of pristine PVA pore-filled PC and GA treated pore-filled PC membranes. As seen from Fig. 2a, the spectrum of pure PVA filled PC membranes resemble that obtained for pure PVA film (Fig. 1b), as PVA form molecular layer on the PC membrane during pore filling procedure so underlying PC characteristics peak may not be observed. FTIR spectra in Fig. 2b–e are associated with GA treated PVA pore-filled membranes. For instance, FTIR spectra of PVA/GA samples reveals two important bands at 2850 and 2750 cm<sup>-1</sup> of C-H stretching related to aldehyde, duplet absorption with peak attributed to the alkyl chain [28]. The O-H stretching vibration peak (region I) from intermolecular and intramolecular hydrogen bonds has decreased and duplet peak (region II) increased

with increase in cross-link time compare to virgin PVA filled PC membrane. This suggests that the hydrogen bonding becomes weaker in GA cross-linked PVA than in virgin PVA because of the diminution in the number of OH groups and increase in acetal formation (as shown in Fig. 3). Also, a strong band from carbonyl group (C=O) was observed at 1720–1740 cm<sup>-1</sup> (region III) and in this region the bands are overlapping and broadening PVA bands for cross-linked membranes. In addition, the C–O stretching at approximately 1100 cm<sup>-1</sup> in uncross-linked membrane has been replaced by a broader absorption band (region IV), which can be attributed to the ether (C–O) and the acetal ring (C–O–C) bands formed by cross-linking reaction of PVA with GA [28] as shown in Fig. 3.

#### 4.3. SEM study for membranes

A SEM micrograph of membrane samples was obtained to study the pore morphology of bare PC substrate before and after the pore filling with PVA. The images in Fig. 4 depict the top-view and the cross-sectional microstructure of bare PC and GA cross-linked PVA pore-filled PC membranes. The cylindrical pores of the membrane are open and visible in bare PC. However, pore-filled PC membrane shows dense cross-sectional structure, which reveals a complete filling of the cylindrical PC pores with PVA. The average thickness of PVA coating layer formed on PC support after pore filling measured by SEM was  $2.3 \pm 0.2 \mu\text{m}$ .

#### 4.4. Ionic conductivity measurement

The voltage drop ( $\Delta U$ ) across the membrane at varying current density ( $I$ ) is shown in Fig. 5. It can be seen that the relationship is linear. The voltage drop is a result of the membrane resistance to charge transport. Thus the change in voltage drop at each corresponding current density value have been used to estimate membrane conductivity values from area resistance of membrane as listed in Table 2. Pristine pore-filled PC membrane shows higher ionic conductivity value than that of GA treated aforementioned membranes. Ionic (hydronium ion) transport occurs by Grōthuss and vehicular mechanisms where the hydronium ion jump from one solvent molecule to the other through hydrogen bonds, or diffuse together with solvent molecules [29]. Pristine PVA filled PC membranes in hydrated form exhibit very loose network structure that easily facilitates the transport of protons through enormous hydrogen bonding. In the case of GA treated PVA membranes, the proton transport channels of polymer matrix tighten more due to cross-links site and diminution of hydroxyl groups that limits swelling and hydrogen bonding site. Moreover, pore-filled PC membrane with pore size of 0.2  $\mu\text{m}$  showed higher proton conductivity compare to 0.01  $\mu\text{m}$  pore size PC membranes filled with

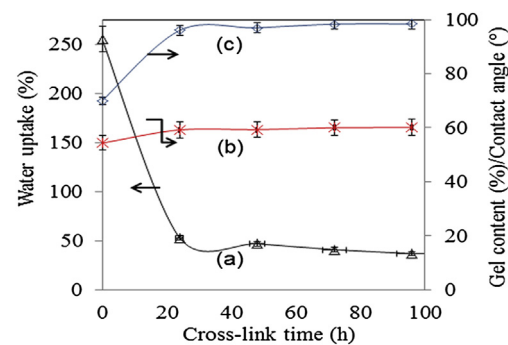


**Fig. 6.** Effects of PVA/GA cross-link time on PEM (a) water uptake (b) contact angle, and (c) gel content.

**Table 2**  
PEMs physicochemical properties.

Membrane	Membrane thickness ( $\mu\text{m}$ )	Range of current density ( $\text{mA cm}^{-2}$ )	Area resistance ( $\Omega \text{cm}^2$ )	Conductivity ( $\text{m}\Omega^{-1} \text{cm}^{-1}$ )
PVAPC0	12.5	0–55	4.2	0.3
PVAPC1	12.3	0–55	4.3	0.29
PVAPC2	12.2	0–55	4.6	0.27
PVAPC3	12.4	0–55	4.9	0.26
PVAPC4	12.3	0–55	5.5	0.23
PVAPC5	8.3	0–55	3.5	0.24
PVAPC6	8.3	0–55	4.8	0.17

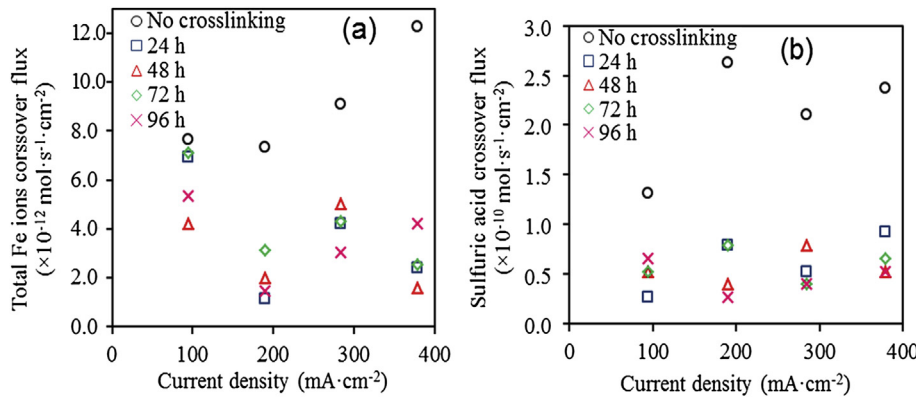


Fig. 7. Effect of current density on crossover of (a) Fe ions, and (b) acid from cathode to anode through PEM.

PVA at same cross-link time of 72 h. This may be due to the fact that the change in membrane area was more restricted for the smaller pore size (0.01  $\mu\text{m}$ ) PC membrane under hydration conditions compare to the larger pore size (0.2  $\mu\text{m}$ ) PC membranes.

#### 4.5. Water uptake, gel content and contact angle

Water uptake is the quantity of water absorbed by the membrane. The water uptake is the amount of water bound to the surface and interstitial sites in the membrane through superficial or hydrogen bonding. The water uptake is the inherent characteristic of PEM that depends upon the types of water attracting functional moiety constituting polymer network and its three-dimensional structure. The presence of water in the membrane typically has a strong effect on the ionic conductivity and mechanical strength. Generally, an excessive water uptake promotes a loss of the mechanical properties whereas shortage of water makes the membranes brittle. However, a too high water uptake can induce significant swelling responsible for a dilution of the ionic groups ( $-\text{OH}$ ) which deteriorates the membranes conductivity. A membrane with high water uptake generally exhibits higher ionic conductivity leading to better fuel cell performances. The high water uptake also complicates the MEA preparation and results in a very low adhesion between the active layer of the electrodes and the membrane.

Herein, the pore filling materials (PVA) is highly hydrophilic and soluble in water due to the formation of enormous hydrogen bonding with water molecules whereas the substrate PC membrane is hydrophobic in nature. Thus in the case of PVA pore-filled PC membranes, the water uptake depends upon the cross-link

density of PVA matrix. Fig 6a presents the degree of water uptake for pore-filled membranes. All the values represent the average of three independent measurements. The uncross-linked membrane exhibited higher water uptake of about 255%, which is five to six times higher than in the membrane cross-linked with GA. Typically the increase of the cross-linking time from 24 h to 96 h resulted in the water uptake decrease from 53% to 37%. Longer reaction time of GA with PVA reduces the hydroxyl content and increases the cross-link density, which decreases the diffusion of water molecules.

As confirmed by FTIR and SEM studies, the pore filling approach of PC membrane with PVA forms a very thin coating layer of PVA on PC surface and makes it hydrophilic. Further, the reactions of PVA with GA induce chemical modification through cross-linking and alter the hydrophilicity of membrane surface. The conversion of hydrophobic PC surface to hydrophilic one (by subsequent treatment with PVA and GA) was confirmed by the decrease in its water contact angle. Since liquid makes contact with the outermost molecular layer of surface, the contact angle is sensitive to the chemical and physical changes occurring on the surface. The average contact angles values measured on membrane's surface are reported in Fig. 6b. The average contact angle obtained on the PC substrate was 91° (not shown here). This value was higher than any studied PVA pore-filled membranes (Fig. 6b) because of its hydrophobic nature. For instance, pure pristine PVAPC0 membrane has showed average contact angle value of 54.3°. Further slight increase in the contact angle was observed with increase in cross-linking time with GA. This fact is attributed to decreases in hydroxyl groups and formation of acetal linkages in polymer matrix. However, pore-filled membranes are still more hydrophilic than the PC substrate.

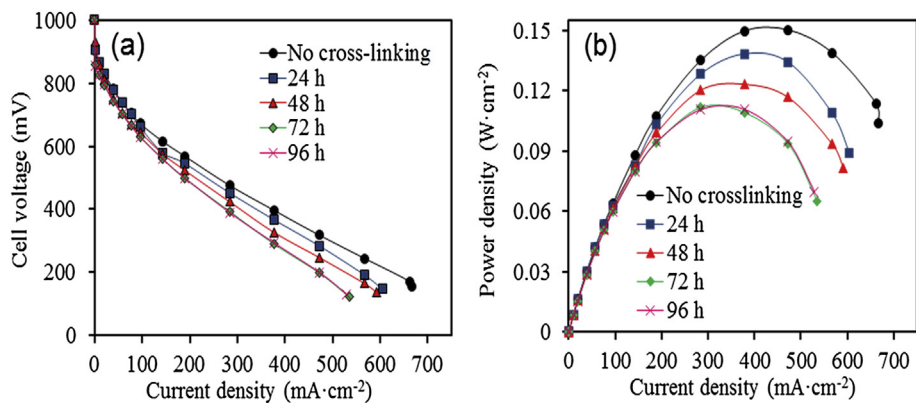
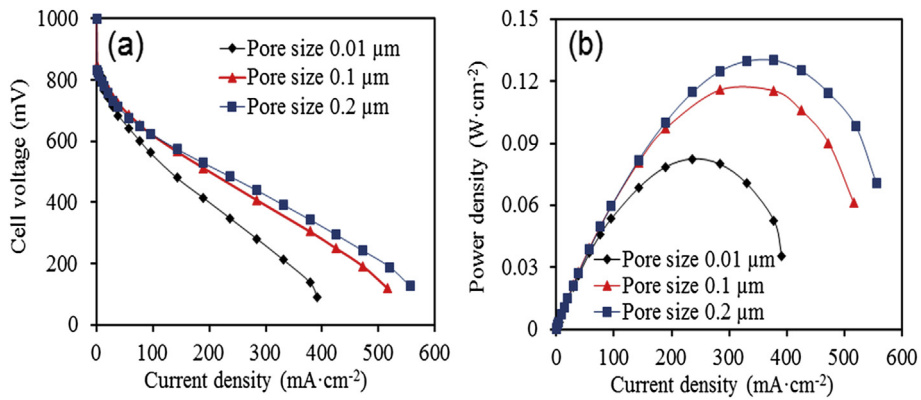


Fig. 8. (a) Cell voltage, and (b) power density vs. current density obtained for cathodic MFC with pristine and GA cross-linked PVA pore-filled PEMs.



**Fig. 9.** (a) Cell voltage, and (b) power density as function of current density for cathodic MFC with GA cross-linked PVA pore-filled PEMs obtained using PC membranes of different pore size (PVA/GA cross-link time 72 h).

The gel content of pore-filled membrane is the dominating parameter that affects the properties of cross-linked PVA in porous substrate. It represents the cross-link fraction of polymer in swollen polymers where uncross-linked polymers leach into solvent. Result showed that the PC membrane was very stable and had contained 99.9% gel after immersing it in 0.1 M sulphuric acid (pH 1) for 7 days at room temperature. Under similar conditions, the measured gel content for all the pore-filled PVA membranes is shown in Fig. 6c. The virgin dried PVAPCO membrane contained only  $63 \pm 5\%$  gel against GA treated PVAPC membranes that showed more than 96% gel. The highest gel content obtained was  $98.3 \pm 0.2\%$  for GA treated membranes for 72 or 96 h. This is due to the formation more stable network because of cross-linking of PVA, which constrains the excessive solvation of polymer matrix.

#### 4.6. Ionic crossover

In cathodic MFCs, the liquid oxidant solution is continuously circulated to the cathode so the measurement of the ionic crossover from cathode to anode is of vital importance. Ionic crossover ( $\text{Fe}^{3+}$ ,  $\text{Fe}^{2+}$  and acid) from cathode to anode produces mixed potential, which results in the drop in cell voltage. The total amount of iron ions ( $\text{Fe}^{3+}$  and  $\text{Fe}^{2+}$ ) and acid crossover at varying current densities have been estimated and shown in Fig. 7a and b respectively for pristine and GA cross-linked PVA pore-filled membranes. Results indicated that the total iron ions and acid crossover were higher in case of pristine PVA pore-filled membrane (PVAPCO) than in the GA cross-linked PVA pore-filled membranes. The GA cross-links PVA and form rigid matrices in the PC pores that restrict the crossover of larger hydrated ions of iron ions and acid. However, it is interesting to note that the value of ionic crossover was independent of the applied current densities as there was no any appreciable concentration difference found for studied iron ions and acid crossover.

#### 4.7. Membrane performance

The performance of cathodic MFC obtained using pristine and GA cross-linked pore-filled membranes are presented by its polarization (current/voltage) curve in Fig. 8a. The polarization curves illustrate the voltage output of the fuel cell for given current density. The results show that the open circuit voltage (OCV) reached 1.0 V. High performance fuel cell membranes exhibit less loss and therefore a higher voltage for a given current load. The power density curves shown in Fig. 8b were produced by multiplying the voltage at each point in the I/V curve by the corresponding current density. The pristine pore-filled membranes show a peak power

density of  $149 \text{ mW cm}^{-2}$  at a current density of  $378 \text{ mA cm}^{-2}$ . As a comparison, at same current density of  $378 \text{ mA cm}^{-2}$ , for GA cross-linked membranes for 24 h, a peak power density has reached at  $138 \text{ mW cm}^{-2}$ . At further increase in the cross-linking time to 96 h, the power density decreased to  $110 \text{ mW cm}^{-2}$ . This is due to the higher water uptake and proton conductivity of pristine pore-filled membranes than GA treated membranes. Overall, ionic crossover is lower in GA treated membranes compare to uncross-linked PVA pore-filled membrane. Our experiments showed that pore-filled membranes produced with different cross-link density (by varying cross-link time with GA) have shown highly reproducible performance characteristics in MFC.

Fig. 9 indicates the effect of the pore size of PC substrate used to prepare pore-filled membranes on fuel cell performance i.e. the I/V versus power density characteristics. The results indicate that the pore-filled membranes prepared using PC substrate having 0.1 and 0.01  $\mu\text{m}$  pore size exhibit lower current density and peak power density than PC having 0.2  $\mu\text{m}$  pore size. This is may be due to the fact that the PC substrate of 0.1  $\mu\text{m}$  and 0.01 produced pore-filled membrane of lower conductivity and lower water uptake.

Fig. 10 shows the cell voltage stability during the fuel cell operation time. GA treated PVA pore-filled membrane (cross-link time 72 h) has operated continuously at constant current loading of  $100 \text{ mA cm}^{-2}$  for 500 h. It should be noticed that the MFC exhibits good performance stability with pore-filled membrane that promises its consistency in cathodic MFC application. The pristine pore-filled PEM contained less than 70% gel and their water uptake was 4–5 times higher than in GA cross-linked membranes. However, the pristine membrane showed very high water crossover due to the excessive water uptake that made it not very appropriate for a continuous operation.

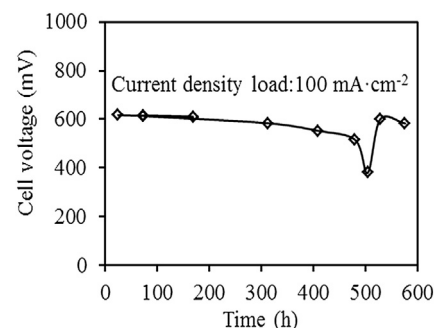


**Fig. 10.** Stability of GA cross-linked PVA pore-filled membrane (cross-link time 72 h) under current load of  $100 \text{ mA cm}^{-2}$ .

## 5. Conclusions

The preparation of PVA pore-filled PC membranes and their properties showed good reproducibility. The MFCs performance of PVA pore-filled membranes strongly depended upon the physico-chemical properties like water uptake, proton conductivity and gel content. Water and hydronium ions (from acids) in polyelectrolyte membrane pores act as a proton transfer medium in MFC. PEMs used for this cathodic MFC application essentially do not require proton exchange site in the polymer matrix as, for example, in Nafion ionomer membrane. Thus, PVA pore-filled PC membranes act as a very good proton transfer medium for MFCs applications with long-term stability.

## Acknowledgments

Financial support was provided by the Ontario Centers for Excellence and the Natural Sciences and Engineering Research Council of Canada. The authors also would like to thank Dr. Vassili Glibin and Mr. Victor Pupkevich for their assistance in obtaining the experimental setup, and Mr. Ian Molnar for assistance in obtaining contact angle measurements. Authors also thank Ying Zhang (Instrumental Analysis Specialist of the Common Laboratory, Western University) for offering FTIR facility.

## References

- [1] Fuel Cell Today, The fuel cell industry review 2012. [www.fuelcelltoday.com](http://www.fuelcelltoday.com). Available at: <http://www.fuelcelltoday.com/analysis/industry-review/2012/the-industry-review-2012>, 5 September 2012 (accessed March 2013).
- [2] Y.-S. Ye, J. Rick, B.-J. Hwang, *Polymers* 4 (2012) 913–963.
- [3] W.H. Philipp, L.-C. Hsu, Three methods for in situ cross-linking of polyvinyl alcohol films for application as ion-conducting membranes in potassium hydroxide electrolyte, NASA Technical Paper 1407, April 1979. Available at: [http://ntrs.nasa.gov/archive/nasa/casi.ntrs.nasa.gov/19790012957\\_1979012957.pdf](http://ntrs.nasa.gov/archive/nasa/casi.ntrs.nasa.gov/19790012957_1979012957.pdf) (accessed March 2013).
- [4] W. Yuhong, H. You-Lo, *J. Appl. Polym. Sci.* 116 (2010) 3249–3255.
- [5] B. Bolto, T. Tran, M. Hoang, Z. Xie, *Progr. Polymer Sci.* 34 (2009) 969–981.
- [6] V. Pupkevich, V. Glibin, D. Karamanov, *J. Power Sources* 228 (2013) 300–307.
- [7] C.-C. Shen, J. Joseph, Y.-C. Lin, S.-H. Lin, C.-W. Lin, B.J. Hwang, *Desalination* 233 (2008) 82–87.
- [8] S. Zeng, L. Ye, S. Yan, G. Wu, Y. Xiong, W. Xu, *J. Membr. Sci.* 367 (2011) 78–84.
- [9] M.S. Kang, J.H. Kim, J.G. Won, S.H. Moon, Y.S. Kang, *J. Membr. Sci.* 247 (2005) 127–135.
- [10] Q. Yang, N. Adrus, F. Tomicki, M. Ulbricht, *J. Mater. Chem.* 21 (2011) 2783–2811.
- [11] H.-L. Lin, T.L. Yu, K.-S. Shen, L.-N. Huang, *J. Membr. Sci.* 237 (2004) 1–7.
- [12] J. Shim, H.Y. Ha, S.-A. Hong, I.-H. Oh, *J. Power Sources* 109 (2002) 412–417.
- [13] T. Yamaguchi, F. Miyata, S.-I. Nakao, *J. Membr. Sci.* 214 (2003) 283–292.
- [14] T. Yamaguchi, H. Zhou, S. Nakazawa, N. Hara, *Adv. Mater.* 19 (2007) 592–596.
- [15] H.-L. Lin, T.L. Yu, L.-N. Huang, L.-C. Chen, K.-S. Shen, G.-B. Jung, *J. Power Sources* 150 (2005) 11–19.
- [16] T. Yamaguchi, F. Miyata, S. Nakao, *Adv. Mater.* 15 (2003) 1198–1201.
- [17] C. Bi, H. Zhang, S. Xiao, Y. Zhang, Z. Mai, X. Li, *J. Membr. Sci.* 376 (2011) 170–178.
- [18] J.-P. Shin, B.-J. Chang, J.-H. Kim, S.-B. Lee, D.H. Suh, *J. Membr. Sci.* 251 (2005) 247–254.
- [19] M.M. Nasef, N.A. Zubir, A.F. Ismail, K.Z.M. Dahlan, H. Saidi, M. Khayet, *J. Power Sources* 156 (2006) 200–210.
- [20] A. Navarro, C. del Río, J.L. Acosta, *Solid State Ionics* 180 (2009) 1505–1510.
- [21] Y. Jin, J.C. Diniz da Costa, G.Q. Lu, *Solid State Ionics* 178 (2007) 937–942.
- [22] D. Karamanov, in: US Patent 7572546 B2, 2009.
- [23] V. Pupkevich, V. Glibin, D. Karamanov, *J. Solid State Electrochem.* 11 (2007) 1429–1434.
- [24] D.G. Karamanov, L.N. Nikolov, V. Mamatakova, *Miner. Eng.* 15 (2002) 341–346.
- [25] D.O. Hummel, E. Scholl, *Atlas of Polymer and Plastics Analysis*, second ed., VCH Verlagsgesellschaft mbH, Weinheim, 1985.
- [26] J.M. Gohil, A. Bhattacharya, P. Ray, *J. Polymer Res.* 13 (2006) 161–169.
- [27] F.L. Martin, in: M.B. Norbert (Ed.), *Encyclopedia of Polymer Science and Technology*, New York, 1971, p. 149.
- [28] H.S. Mansur, R.L. Orifice, A.A.P. Mansur, *Polymer* 45 (2004) 7193–7202.
- [29] T. Uma, *RSC Advan.* 2 (2012) 6752–6755.